Lespedeza homoloba enhances the immunosuppressive milieu of adipose tissue and suppresses fasting blood glucose

KYOKO KOBAYASHI, AIRI TANABE and KENROH SASAKI

Division of Pharmacognosy, Faculty of Pharmaceutical Sciences, Tohoku Medical and Pharmaceutical University, Sendai, Miyagi 981-8558, Japan

Received June 10, 2024; Accepted August 19, 2024

DOI: 10.3892/br.2024.1852

Abstract. Immune cells migrate to hypertrophied adipocytes and release proinflammatory cytokines, leading to adipocyte dysfunction and diabetes. Numerous species of *Lespedeza*, which are members of the plant family Fabaceae and distributed primarily in temperate Asia and North America, exhibit binding to peroxisome proliferator-activated receptor (PPAR) γ, a target nuclear receptor for treating diabetes. Therefore, the present study aimed to determine which species of *Lespedeza* plants exert an anti-inflammatory effect in adipose tissue and suppression of blood glucose increase through PPARγ ligand and radical scavenging activity. PPARγ binding and DPPH radical scavenging assays of *L. homoloba* (LH), *L. thunbergii* (LT), *L. maximowiczii* (LM) and *L. thunbergii* (LT) were performed. LH and LT showed significant ligand activity towards PPARγ and notable radical scavenging activity. LH exhibited a stronger DPPH radical scavenging activity than LT and thus was measured adiponectin secretion from 3T3-L1-derived adipocytes and IL-10 secretion from murine splenocytes. LH increased the adiponectin and the IL-10 secretions. In flow cytometric analysis, BALB/c male mice administered LH exhibited an increase in regulatory T cells (Tregs) and cytotoxic T lymphocyte-associated protein (CTLA)-4$^+$ Tregs as well as a decrease in T helper (Th)17, Th17/Treg ratio and CD8$^+$ and CD4$^+$ T cells in subcutaneous adipose tissue. Conversely, in the spleen, LH decreased Tregs and increased Th17 cells, Th17/Treg ratio and CD4$^+$ and CD8$^+$ T cells. These findings indicated that LH activated immunoreaction in the spleen and Treg cells that migrate to subcutaneous adipose tissue may suppress inflammation. In fasting blood glucose and adiponectin assays, LH-exposed mice exhibited suppression of fasting glucose levels. Therefore, LH may prevent type 2 diabetes by suppressing adipose tissue inflammation.

Correspondence to: Professor Kyoko Kobayashi, Division of Pharmacognosy, Faculty of Pharmaceutical Sciences, Tohoku Medical and Pharmaceutical University, 4-1 Komatsushima 4-Chome, Aoba-Ku, Sendai, Miyagi 981-8558, Japan
E-mail: k-kyoko@tohoku-mpu.ac.jp

Key words: Lespedeza homoloba, regulatory T cell, CTLA-4, Th17, adipose tissue

Introduction

During adipocyte hypertrophy, macrophages infiltrate adipose tissue following the biogenesis of adipocytes (1). Macrophages secrete proinflammatory cytokines that induce adipose tissue inflammation, which causes insulin resistance (2). Adipose tissue-specific insulin-resistant mouse models accumulate proinflammatory macrophages in the adipose tissue (3,4). Nuclear receptor peroxisome proliferator-activated receptor (PPAR)γ, which is abundantly expressed in adipose tissue and macrophages, is a target receptor for thiazolidine antidiabetic agents and contributes to adipogenesis and antiinflammation in adipose tissue. The activation of PPARγ inhibits the secretion of several cytokines, such as tumor necrosis factor-α (TNF-α), interferon-γ, interleukin (IL)-1, IL-6 and transforming growth factor-β (TGF-β), in adipose tissue (5). Foxp3$^+$ regulatory T cells (Tregs), which serve an important role in obesity, migrate to inflamed non-lymphoid tissue, such as adipose tissue, and suppress the function of proinflammatory T cells (6).

Flavonoids, which possess several hydroxyl groups in their diphenylpropane structure, generally exert anti-inflammatory effects due to multiple phenolic hydroxyl groups with radical-scavenging ability (7). However, their bioavailability is low, because of their hydrophilic properties (8). Our unpublished study found that prenylflavonoids, which possess a C5 isoprenoid unit in a diphenylpropane structure, have a negligible effect on radical scavenging activity but exhibit stronger PPARγ ligand activity than general flavonoids such as quercetin, which is widely found in plants. Moreover, increased prenylflavonoid accumulation and decreased efflux from cells have been reported because the C5 isoprenoid unit increases hydrophobicity of the diphenylpropane structure to enhance its affinity for the cell membrane (9) compared with non-prenylated flavonoids, such as quercetin and naringenin. Prenylflavonoids are present in the genus *Lespedeza* which belongs to the family Fabaceae and is distributed throughout East Asia. The biological activities of *Lespedeza* plants include anti-inflammatory (10), antidiabetic (11), anti-tyrosinase (12), antibacterial and antitumor activities (13) and nitric oxide production (14). Therefore, the present study

aimed to determine which *Lespedeza* sp. among four species, namely *L. buergeri* (LB), *L. homoloba* (LH), *L. maximowiczii* (LM) and *L. thunbergii* (LT), that contain prenylflavonoids exhibit PPARγ ligand activity and the accumulation of Tregs in adipose tissue to induce anti-inflammatory effects and suppress blood glucose levels.

Materials and methods

Animals. A total of 54 5-week-old BALB/c male mice (weight 19-20 g) were purchased from Japan SLC, Inc. (Hamamatsu, Japan) and housed under standardized conditions (temperature, 25±1˚C; humidity, 55±5%) in a room with a 12/12-h light/dark cycle. The mice were fed standard chow (cat. no. CE-2, CLEA Japan, Inc.) and water and acclimatized to the room for 1 week. All animal experiments were approved by Animal Experimental Committee of Tohoku Medical and Pharmaceutical University (Sendai, Japan (approval no. 23032-a) and performed in accordance with the ethical guidelines of the university. Euthanasia of mice was performed to adhere to the American Veterinary Medical Association Guidelines for the Euthanasia of Animals (15). The mice were euthanized by excessive inhalation of 5% isoflurane in a chamber; cardiac and respiratory arrest were confirmed and then the tissues were resected for analysis.

Extraction of samples. *Lespedeza sp*. were provided by Sendai Wild Plants Garden under the jurisdiction of Sendai City Office Construction Bureau Park Management Section. These plants were air-dried and extracted with 20-fold methanol volume of plant weight at room temperature for 7 days. The methanol extract was filtered and concentrated by a rotary evaporator under reduced pressure at 40˚C to obtain the dried extract. The yields of LB, LH, LM and LT-dried extracts were 94.35, 64.13, 79.17 and 51.72 mg/g, respectively.

PPARγ binding assay. PPARγ binding assay was conducted using the method described by Konno *et al* (16). Briefly, 0.2 μg per well CREB binding protein (CBP; BIOSS) was immobilized in the wells of a plastic 96-well plate at 37˚C for 1 h. After blocking with 5% skimmed milk at 37˚C for 1 h, PPARγ (PPARγ Human Recombinant, ProSpec-Tany TechnoGene Ltd.) was immobilized on the CBP in at 37˚C for 1 h. After the washing with wash buffer (0.1 M PBS containing 0.05% Tween 20), methanol extracts of *Lespedeza sp*. (the reaction concentrations: 0.038, 0.075, 0.15, 0.3 mg/ml) or pioglitazone (the reaction concentrations: 0.001, 0.01, 0.1, 1 μM) were added, respectively, and the plate was incubated for 1 h at 37˚C. 500-fold diluted PPARγ antibody (rabbit polyclonal, cat. No. AHP1269, Bio-Rad Laboratories, Inc.) was added to the wells after washing with the wash buffer and then incubated for 1 h at 37˚C. 40-fold diluted alkaline phosphatase-conjugated IgG antibody (goat anti-rabbit, catalog No. 170-6581, Bio-Rad Laboratories, Inc.) was added after the wells washing with the wash buffer and then incubated for 1 h at 37˚C. Following shaking with a microplate shaker at room temperature in the dark for 20 min, absorbance of the wells was measured at 405 nm with a spectrophotometer. The PPARγ binding activity was calculated using the following formula: PPARγ binding activity=absorbance of sample/absorbance of control. Pioglitazone (FUJIFILM Wako Pure Chemical Corporation) was used as a positive control.

DPPH radical scavenging assay. DPPH radical scavenging assay was conducted using the method by Blois (17). Briefly, 100 mM (pH 5.5) acetate buffer, ethanol (95 vol%), 500 μM DPPH ethanol solution and sample solution (6.25, 125, 250, 500, 1,000, 2,000 μg/ml) or Trolox (0.25, 0.5, 1.0, 2.0 μM), respectively, were mixed in the same tube (1.00 and 1.25 ml and 250.00 and 50.00 μl, respectively). The mixture was incubated at room temperature for 30 min in the dark and absorbance was measured at 517 nm with a spectrophotometer. DPPH radical scavenging activity was calculated using the following formula: [(Absorbance of control-absorbance of sample)/absorbance of control] x100. Trolox (Tokyo Chemical Industry Co., Ltd.) was used as a positive control.

Splenocyte preparation. The spleen of male BALB/c mice was extirpated under sterile conditions following euthanasia via inhalation of isoflurane. The spleen was minced by scissors and ground by slide glass in RPMI-1640 medium (FUJIFILM Wako Pure Chemical Corporation) and filtered through a 40-μM mesh. The cell suspension was hemolyzed using 1X RBC Lysis Buffer, pluriSelect Life Science) to obtain splenocytes. The splenocytes were suspended in RPMI-1640 containing 0.05 mM 2-mercaptoethanol (FUJIFILM Wako Pure Chemical Corporation), 10% heat-inactivated FBS (Thermo Fisher Scientific, Inc.) and Antibiotic-Antimycotic Mixed Stock Solution (100X; Nacalai Tesque, Inc.).

Splenocyte toxicity. A total of $5x10^4$ splenocytes and 4 μg concanavalin A (derived from *Canavalia esiformis;* Merck KGaA) were added to the individual wells of a 96-well plate and incubated at 37˚C in a humidified atmosphere containing 5% CO_2 for 48 h. The medium was exchanged for RPMI-1640 medium containing LH and incubated at 37˚C in a humidified atmosphere containing 5% CO_2 for 48 h. The splenocyte proliferative activity was determined by adding Cell Count Reagent SF (Nacalai Tesque, Inc.) and incubating for 4 h at 37˚C in a humidified atmosphere containing 5% CO_2 and measuring the absorbance at 450 nm with a spectrophotometer.

IL-2 secretion from cultured murine splenocytes. A total of $5x10^6$ splenocytes and 4 μg concanavalin A were added to the individual wells of a 24-well plate. The plate was incubated at 37˚C in a humidified atmosphere containing 5% CO_2 for 48 h. The medium was exchanged for RPMI-1640 medium containing LH and incubated at 37˚C in a humidified atmosphere containing 5% CO_2 for 48 h. The medium in the individual wells was collected and stored at -80˚C until measurement of the IL-2 concentrations in the medium using an ELISA kit (Mouse IL-2 Quantikine ELISA kit, cat. no. DY402-05, R&D Systems, Inc.) according to the manufacturer's instructions.

3T3-L1 cell culture. Medium-low-glucose DMEM (Merck KGaA) containing 10% FBS, isobutyl-methylxanthine (IBMX), dexamethasone (DEX) and insulin (all FUJIFILM Wako Pure Chemical Corporation) and Antibiotic-Antimycotic

Mixed Stock Solution were used for cell culture at 37˚C in a humidified atmosphere containing 5% CO_2.

3T3-L1 cell differentiation. 3T3-L1 cells, a fibroblast isolated from the embryo of a mouse, were purchased from the Japanese Collection of Research Bioresources Cell Bank (National Institutes of Biomedical Innovation, Health, and Nutrition, Ibaraki, Japan). 3T3-L1 cell cultivation and differentiation were performed using a previously described method (18). 3T3-L1 cells at the 7th passage were cultured at 37˚C with 5% CO_2 in DMEM supplemented with 10% FBS and antibiotic/antimycotic. To individual wells of a 24-well plate, $3x10^4$ cells/well were seeded and the plate was incubated for 48 h in maintenance medium (10% FBS and 1% antibiotic/antimycotic in DMEM) at 37˚C in a humidified atmosphere containing 5% CO_2. After reaching 90% confluence, the medium was changed to differentiation induction medium (0.5 mM IBMX and 1.0 μM DEX in the maintenance medium) and incubated at 37˚C for 48 h in a humidified atmosphere containing 5% CO_2. The medium was replaced with differentiation medium (1.7 μM insulin in the maintenance medium) and incubated at 37˚C for 48 h in a humidified atmosphere containing 5% CO_2.

Oil Red O (ORO) staining and adiponectin secretion determination. 3T3-L1-derived adipocytes were used to determine the lipid accumulation and adiponectin secretion values. After the 3T3-L1 cell differentiation, the medium was replaced with maintenance medium containing samples (0.00001, 0.0001, 0.001, 0.01 mg/ml) or pioglitazone (0.28, 2.8, 28, 280 μM), respectively, and incubated for 96 h (medium was changed every 48 h) at 37˚C in a humidified atmosphere containing 5% CO_2. Medium in the individual wells was collected and stored at -80˚C until use for the determination of the adiponectin level using the ELISA kit (Mouse adiponectin/Acrp30 DuoSet® ELISA, cat. No. DY1119-05, R&D Systems, Inc.) according to the manufacturer's instructions. Cells were fixed with 10% formaldehyde for 1 h at room temperature. Following incubation in 2-propanol for 1 min at room temperature, the lipid droplets in the cells were stained with 3 mg/ml ORO in 60% 2-propanol solution for 20 min at room temperature. After washing with 60% 2-propanol, 4% triton-X-100/2-propanol solution was added to the well for 5 min at room temperature to extract ORO in lipid droplets of adipocytes. The absorbance of the extracted solution was measured at 492 nm with a spectrophotometer and the lipid accumulation value was quantified using an ORO standard curve. Pioglitazone (FUJIFILM Wako Pure Chemical Corporation) was used as a positive control.

Cytokine secretion assay. A total of 12 6-week-old male BALB/c mice were divided into three groups (n=4/group) and allowed free access to 0.1% water solution of methanol extract of LH or LT for 14 days. Four days later, mice were subcutaneously injected with 50 μl 1 mg/ml concanavalin A suspended in complete Freund's adjuvant (Merck KGaA) through the tail to stimulate T cells. After 7 days, splenocytes were prepared as aforementioned. A total of $5x10^6$ splenocytes and 4 μg concanavalin A were added to the individual wells of a 24-well plate. The plate was incubated at 37˚C in a humidified atmosphere containing 5% CO_2. The medium in the individual wells was collected following 25 and 50 h of incubation and stored at -80˚C until measurement of the IL-10, IL-17 and TNF-α concentrations in medium using an ELISA kit (Mouse IL-10, cat. no. DY417-05, IL-17, cat. No. DY421-05, and TNF-α, cat. No. DY410-05, Quantikine ELISA kits, respectively, R&D Systems, Inc.) according to the manufacturer's instructions.

Fasting blood glucose and adiponectin levels. A total of 15 6-week-old male BALB/c mice were divided into three groups (n=5/group) and allowed free access to 0.1% or 0.2% water solution of methanol extract of LH to 0.1% LH-loaded group or 0.2% LH-loaded group for 14 days, respectively, to determine the dose-dependent effect of LH. To determine low-(0.1%) and high-dose (0.2%) concentrations of LH, voluntary water intake/day of mice was observed so that the mice ingested 100 or 200 mg/day sample extract. After fasting for 15 h, the blood glucose levels of mice in the tail vein were measured using a blood glucose meter and test paper (ACCU-CHECK® Aviva Strip, Roche Diagnostics Co., Ltd.). After mouse euthanasia, the blood was collected from the heart by heparin-treated syringe and centrifuged at 15,000 x g for 5 min at room temperature to obtain plasma and adiponectin concentration was measured using an ELISA kit (Mouse adiponectin/Acrp30 DuoSet® ELISA, cat. No. DY1119-05, R&D Systems, Inc.) according to the manufacturer's instructions.

Flow cytometry sample preparation. A total of 15 6-week-old male BALB/c mice were divided into three groups (n=5/group) and allowed free access to 0.1% or 0.2% water solution of LH for 14 days. Furthermore, obese 13-week-old male BALB/c mice established by the administration of high-fat diet (D12492, RESEARCH DIETS Inc.) were divided into two groups (n=6/group) and allowed free access to 0.1% water solution of LH for 30 days. Four days later, the mice were subcutaneously injected with 50 μl 1 mg/ml concanavalin A in complete Freund's adjuvant (Merck KGaA) through the tail to stimulate T cells. After 7 days, spleen and subcutaneous fat were extirpated under sterile conditions following mouse euthanasia via inhalation of isoflurane. The splenocytes were prepared as aforementioned. The subcutaneous fat was minced in RPMI-1640 medium containing 0.5% collagenase type 4 (Worthington Biochemical Corporation) using dissecting scissors. After incubation at 37˚C for 30 min under shaking, DMEM containing 2% FBS was added to further mince the tissue by pipetting and filtered through a 40-μM mesh. The tissue suspension was centrifuged at 800 x g for 5 min at room temperature to separate the adipocyte and the stromal vascular cell fraction. Lymphocytes were isolated from stromal vascular cells using Lympholyte®-M Cell Separation Media (Cedarlane).

Cell staining and flow cytometric analysis. Splenocytes and lymphocytes isolated from stromal vascular cell fraction were fixed and permeabilized using Fixation/Permeabilization Concentrate and Diluent kit (Thermo Fisher Scientific, Inc.) according to the manufacturer's instructions and which divided into 100 μl to four tubes (tubes A-D). To analyze the percentage of $CD4^+$ cells in the lymphocytes, the splenocytes or the lymphocytes in Tube B were stained with 180-fold diluted Super Bright 600-conjugated CD4 antibody [monoclonal (RM4-5), Super Bright™ 600, eBioscience™,

cat. no. 63-0042-82, Thermo Fisher Scientific Inc.]. To analyze the percentage of Tregs ($CD4^+$ $CD25^+$ $Foxp3^+$ T cells), IL-10^+ Tregs ($CD4^+$ $Foxp3^+$ IL-10^+ T cells), cytotoxic T-lymphocyte antigen (CTLA)-4^+ Tregs ($CD4^+$ $Foxp3^+$ CTLA-4^+ T cells) and T helper (Th)17 ($CD4^+$ IL-$17A^+$ T cells), the splenocytes or the lymphocytes in Tube C were stained with 180-fold diluted Super Bright 600-conjugated CD4 (cat. no. 63-0042-82) and 160-fold diluted PE-Cyanine5-conjugated CD25 antibody [CD25 monoclonal antibody (PC61.5), PE-Cyanine5, cat. no. 15-0251-82)], 20-fold diluted Alexa Fluor 488-conjugated Foxp3 [(cat. no. 53-4774-42)], 80-fold diluted Alexa Fluor 700-conjugated IL-10 [IL-10 monoclonal antibody (JES5-16E3), Alexa Fluor 700, cat. no.56-7101-82)], 80-fold diluted phycoerythrin-conjugated CTLA-4 antibody [CD152 (CTLA-4 monoclonal antibody (UC10-4B9), PE, cat. no. 12-1522-82] and 80-fold diluted eFluor 450-conjugated IL-17A antibody [IL-17A monoclonal antibody (eBio17B7), eFluor 450, cat. no. 48-7177-82; all eBioscience™, Thermo Fisher Scientific, Inc.]. To analyze the percentage of $CD8^+$ T cells in the lymphocytes, the splenocytes or the lymphocytes in Tube D were stained with 80-fold diluted Super Bright 702-conjugated CD8 antibody (cat. no. 67-0081-82; Thermo Fisher Scientific, Inc.). The splenocytes or the lymphocytes in Tube A were not stained. These tubes were incubated on ice for 1 h. Flow cytometric analysis was conducted using Attune NxT Acoustic Focusing Cytometer and the data were analyzed using the Attune NxT Software version 2.6 (Thermo Fisher Scientific, Inc.).

High performance liquid chromatography (HPLC). Methanol extracts of LH and LT were sonicated with methanol at 40 kHz, 40˚C for 1 h and filtrated through a 0.45-μm filter membrane to obtain solutions with a concentration of 1 mg/ml. Formononetin (0.05 mg/ml) was purchased from Tokyo Chemical Industry Co., Ltd. Lespedezaflavanone H (0.025 mg/ml) was gifted by Professor Toshio Miyase, School of Pharmaceutical Sciences, University of Shizuoka (Shizuoka, Japan). HPLC analysis of methanol extracts of LH and LT was performed by LC-20AD Solvent delivery unit (Shimadzu Scientific Instruments) with COSMOSIL 5PE-MS packed column (4.6x250.0 mm, 5 μm particle size), column oven (cat. no. CO631C, GL Sciences) and UV detector (UV-VIS detector S-3170, Soma Optics, Ltd.). Analysis was performed using the following conditions: Mobile phase, acetonitrile:water=60:40; flow rate, 1 ml/min; detection wavelength, 214 and 280 nm; injection volume, 10 μl and column temperature, 40˚C. The peak areas were analyzed by Chromato-PRO version 5.0.0.199 (Runtime Instruments Co., Ltd.).

Statistical analysis. Statistical analysis was conducted using the SigmaStat statistical software ver. 2.03 (SPSS Inc.). Student's unpaired t test, and one-way ANOVA followed by Dunnett's multiple comparison or Bonferroni's test were performed for comparisons. $P<0.05$ was considered to indicate a statistically significant difference. Data are represented the mean ± SD of two independent experiments.

Results

LH exhibits PPARγ binding and radical scavenging activity. PPARγ binding activity of LB, LH, LM, and LT was determined by ELISA. Pioglitazone, a PPARγ agonist, had significant binding activity on PPARγ (Fig. 1A). LB had significantly reduced PPARγ binding activity at 0.038, 0.150, 0.300 mg/ml. LM exhibited no change in binding activity; LH exhibited a significant increase at 0.300 but decrease in 0.038 mg/ml compared with that of the control. LT had significantly increased binding activity at 0.075-0.300 mg/ml (Fig. 1B). Trolox exhibited a dose-dependent increase in DPPH radical scavenging activity (Fig. 1C). LH and LT exhibited a dose-dependent increase in these DPPH scavenging, with LH having a stronger radical scavenging activity than LT at 6.25-500.00 μg/ml (Fig. 1D).

LH suppresses IL-2 secretion from splenocytes. PPARγ expression in T cells decreases the production of inflammatory cytokines (19). To investigate whether PPARγ-agonistic LH suppressed the production of inflammatory cytokine IL-2, murine splenocytes were incubated with LH, and the splenocyte toxicity and IL-2 secretion from splenocytes were assessed. Splenocyte toxicity was not observed in the presence of LH whereas LH showed significant proliferation of splenocytes at 0.0625 and 0.1250 compared with that at 0 mg/ml (Fig. 1E). IL-2 secretion from splenocytes was evaluated following the addition of LH. LH significantly suppressed IL-2 secretion at 0.15625 mg/ml compared with the control (Fig. 1F).

LH increases lipid accumulation and adiponectin secretion of 3T3-L1-derived adipocytes. Activating of PPARγ expressed in adipocytes increases lipid accumulation (20) and adiponectin secretion (21). Therefore, LH and LT, which showed PPARγ binding activity, were evaluated for lipid accumulation and adiponectin secretion of 3T3-L1-derived adipocytes. Pioglitazone, significantly decreased lipid accumulation at 0.28 μM (Fig. 2A). LH exhibited significantly increased lipid accumulation at 0.00001 and 0.00100 mg/ml, whereas LT showed significantly increased accumulation at 0.00100 mg/ml (Fig. 2B). Pioglitazone significantly increased adiponectin concentration at 28-280 μM (Fig. 2C). Furthermore, LH showed increased adiponectin concentration at 0.00001-0.00100 mg/ml (Fig. 2D).

LH promotes IL-10secretion from splenocytes. To determine whether LH and LT influence the levels of anti-inflammatory cytokine IL-10 as well as proinflammatory cytokines IL-17 and TNF-α secreted from the spleen, splenocytes of 0.1% LH- or LT-exposed mice were cultured. At 25 h, the splenocytes of 0.1% LH-exposed mice exhibited significantly increased IL-10 levels, whereas those of 0.1% LT-exposed mice exhibited significantly decreased IL-10 levels (Fig. 3A). Furthermore, splenocytes of LH- and LT-exposed mice exhibited decreased IL-17 levels, but the decrease was had not significant (Fig. 3B). Similarly, splenocytes of 0.1% LH-exposed mice decreased exhibited TNF-α levels, but the decrease was not significant (Fig. 3C).

LH suppresses fasting blood glucose but does not affect blood adiponectin levels. PPARγ agonists increase levels of glucose transporter (GLUT)-4 in adipocytes of peripheral tissues such as muscle and liver to facilitate glucose uptake (22) and promote translocating fatty acids in the

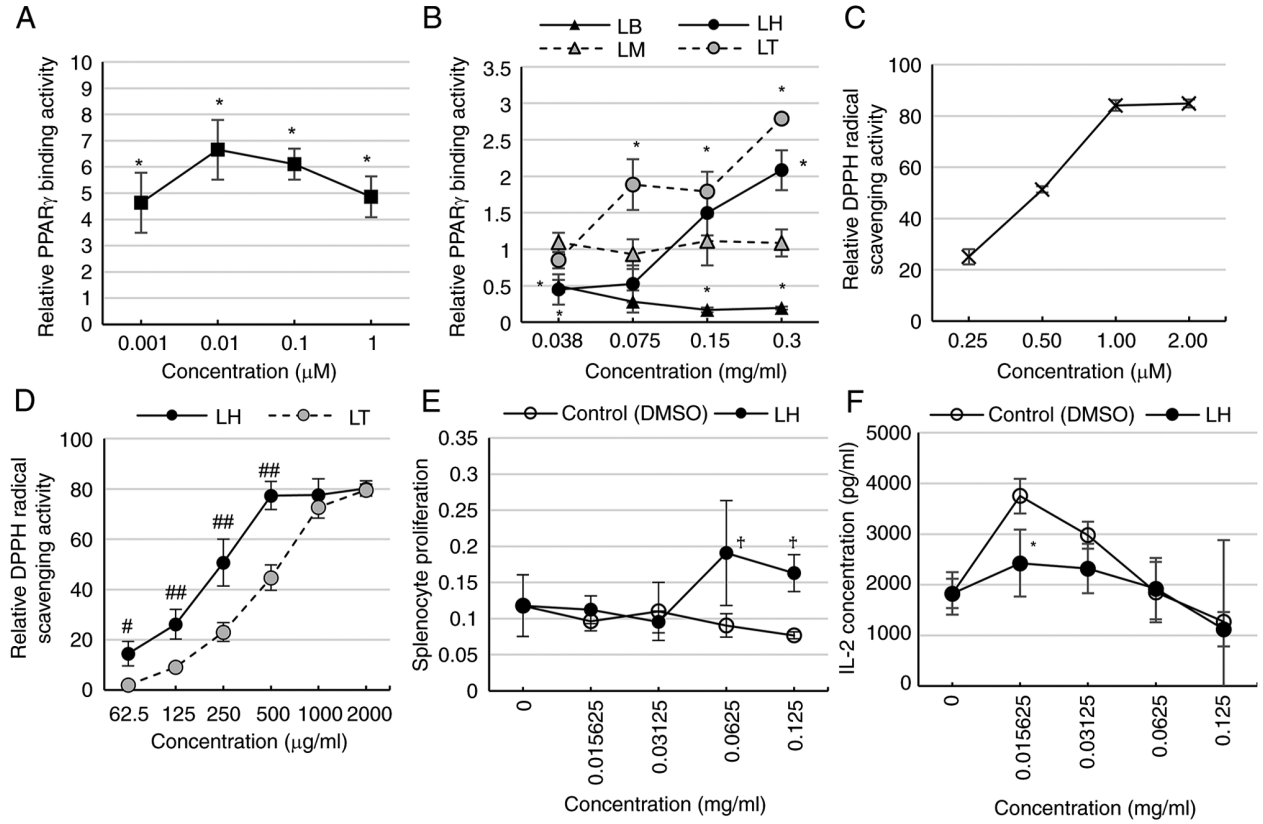

Figure 1. Comparison of PPARγ binding and radical scavenging activity. (A) PPARγ binding activity of pioglitazone (positive control). (B) Comparison of PPARγ binding activity among LB, LH, LM, and LT. (C) DPPH radical scavenging activity of Trolox (positive control). (D) Comparison of DPPH radical scavenging activities between LH and LT. (E) Splenocyte toxicity of LH. No significant differences between LH and the control were observed. (F) IL-2 secretion of LH from splenocytes. *P<0.05 vs. control, #P<0.05, ##P<0.01 vs. LT, †P<0.05 vs. 0 mg/ml. LB, *Lespedeza buergeri*; LH, *Lespedeza homoloba*; LM, *Lespedeza maximowiczii*; LT, *Lespedeza thunbergii*.

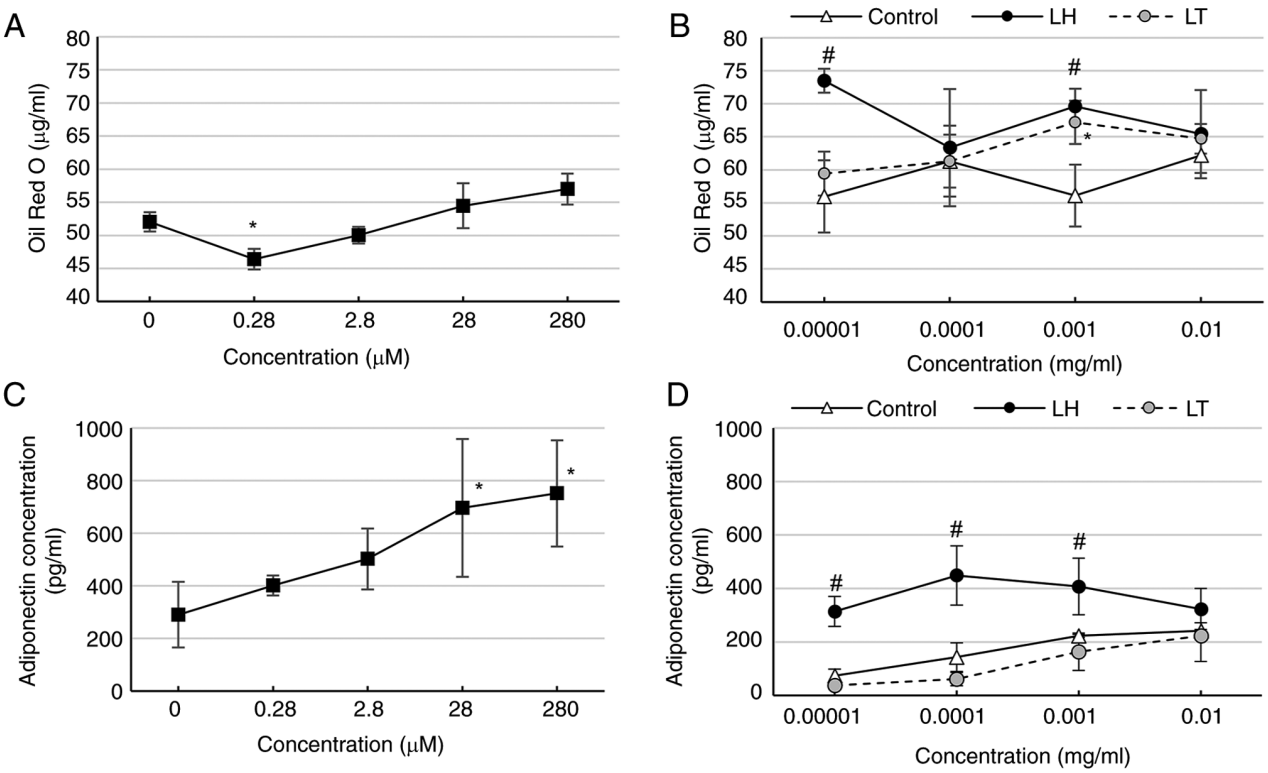

Figure 2. Lipid accumulation and adiponectin secretion of 3T3-L1-derived adipocytes. Lipid accumulation in 3T3-L1-derived adipocytes supplemented with (A) pioglitazone as positive control, (B) LH and LT. Adiponectin secretion from 3T3-L1-derived adipocytes supplemented with (C) pioglitazone and (D) LH and LT. *P<0.05 vs. 0 mg/ml, #P<0.05 vs. control. LH, *Lespedeza homoloba*; LT, *Lespedeza thunbergii*.

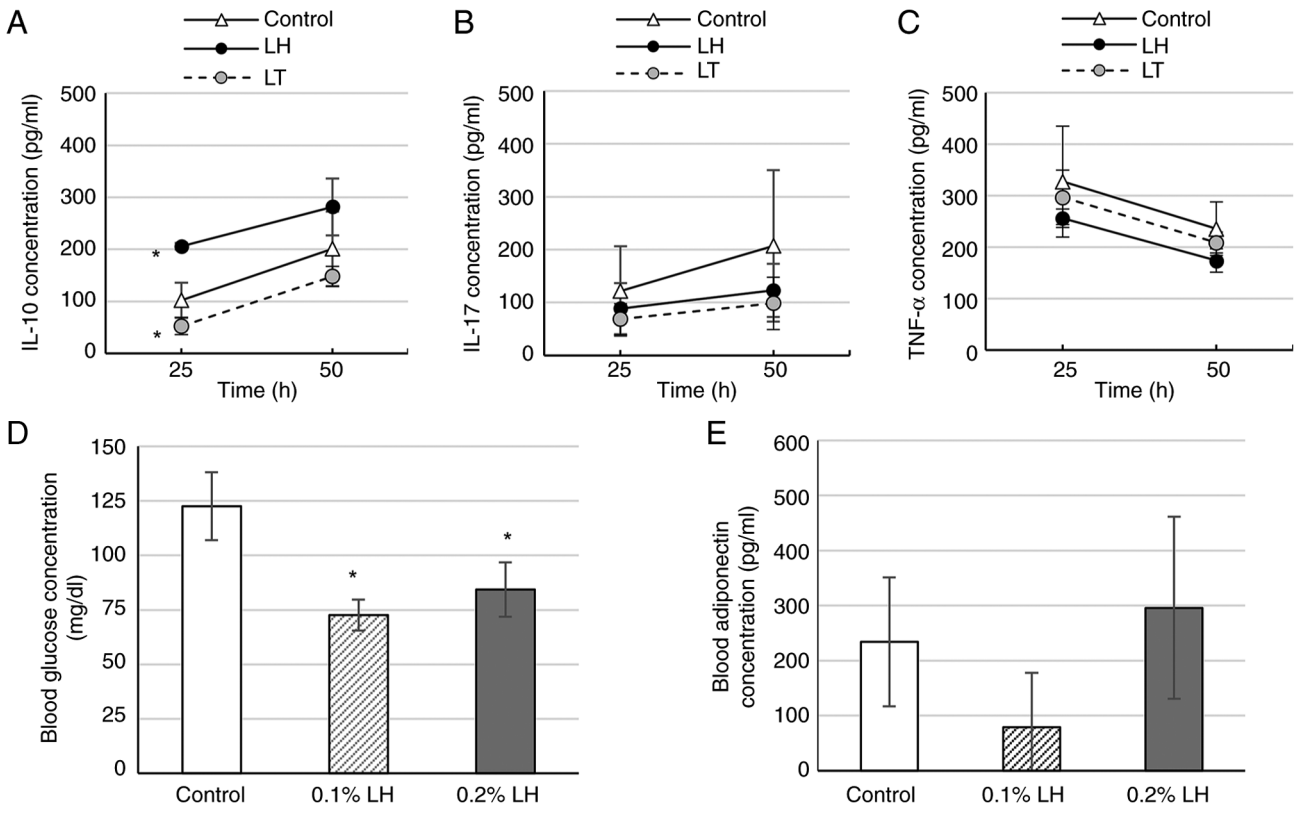

Figure 3. Cytokine secretion from mice splenocytes, fasting blood glucose and adiponectin levels. (A) IL-10, IL-17A, and TNF-α secretions from the splenocytes of LH- or LT-exposed BALB/c male mice. (B) LH- and LT-exposed mice showed a decreasing trend of IL-17 secretion. (C) LH-exposed mice showed a decreasing trend of TNF-α secretion. (D) blood glucose and (E) adiponectin levels after 15 h fasting. *P<0.05 vs. control. LH, *Lespedeza homoloba*; LT, *Lespedeza thunbergii*.

peripheral tissues to adipose tissues, leading to suppression of blood glucose levels (23). In white adipose tissue, PPARγ agonists promote adiponectin transcription, synthesis and secretion (21). Therefore, it was determined whether LH, which exerted PPARγ agonistic activity, affects blood glucose and adiponectin levels. Mice exposed to 0.1 and 0.2% LH exhibited significantly decreased fasting blood glucose levels compared with the control mice (Fig. 3D). 0.1% LH-exposed mice showed lower fasting adiponectin levels whereas 0.2% LH-exposed mice showed higher fasting blood adiponectin levels than the control mice, but these levels were not significantly different (Fig. 3E).

LH-exposed mice exhibit decrease Th17/Treg in subcutaneous adipose tissue. To determine whether Tregs essential for suppressing adipose tissue inflammation were increased in subcutaneous fat of mice, the percentage of $CD25^+$ $Foxp3^+$ Tregs in the $CD4^+$ T cell population was analyzed via flow cytometry (Fig. 4A). Th17 cells mutually maintain a balance with Tregs to regulate the immune system (24); therefore, the percentage of IL-$17A^+$ $CD4^+$ Th17 cells in $CD4^+$ T cells was analyzed via flow cytometry (Fig. 4B). Mice exposed to 0.1% LH had significantly increased Tregs but there was no effect in mice exposed to 0.2% LH compared with the control (Fig. 4C). Although mice exposed to 0.2% LH exhibited significantly decreased Th17 cells and Th17/Treg ratio, 0.1% LH exhibited no significant decrease in Th17 cells and Th17/Treg ratio compared with control mice (Fig. 4D).

LH-exposed mice exhibit increase Th17/Treg in the spleen. The proportion of $CD25^+$ $Foxp3^+$ and IL-$17A^+$ $CD4^+$ T cells was analyzed (Fig. 5A and B). Mice exposed to 0.1 and 0.2% LH had significantly decreased Tregs compared with the control (Fig. 5C). Mice exposed to 0.2% LH exhibited significantly increased Th17 cells (Fig. 5D), whereas mice exposed to 0.1 and 0.2% LH had significantly increased Th17/Treg ratio (Fig. 5E).

LH-exposed mice exhibit suppress IL-10^+ Tregs in the spleen. To determine whether LH creates an immunosuppressive milieu in subcutaneous adipose tissue by increasing suppressive cytokine IL-10 secretion from Tregs of the adipose tissue, IL-10^+ Tregs in subcutaneous adipose tissue and spleen were analyzed via flow cytometry (Fig. 6A and B). No significant difference was observed in IL-10^+ Tregs in subcutaneous adipose tissue (Fig. 6C); however, in the spleen, mice exposed to 0.1 and 0.2% LH exhibited significantly decreased IL-10^+ Treg levels (Fig. 6D).

LH-exposed mice increase CTLA-4^+ Tregs in the subcutaneous adipose tissue. To determine whether LH creates an immunosuppressive milieu in the subcutaneous adipose tissue by increasing CTLA-4 expression on Tregs to induce antigen-presenting cell (APC) dysfunction, CTLA-4^+ Tregs in the subcutaneous adipose tissue and spleen were analyzed via flow cytometry (Fig. 7A and B). Mice exposed to 0.1% LH exhibited significantly increased CTLA-4^+ Treg levels

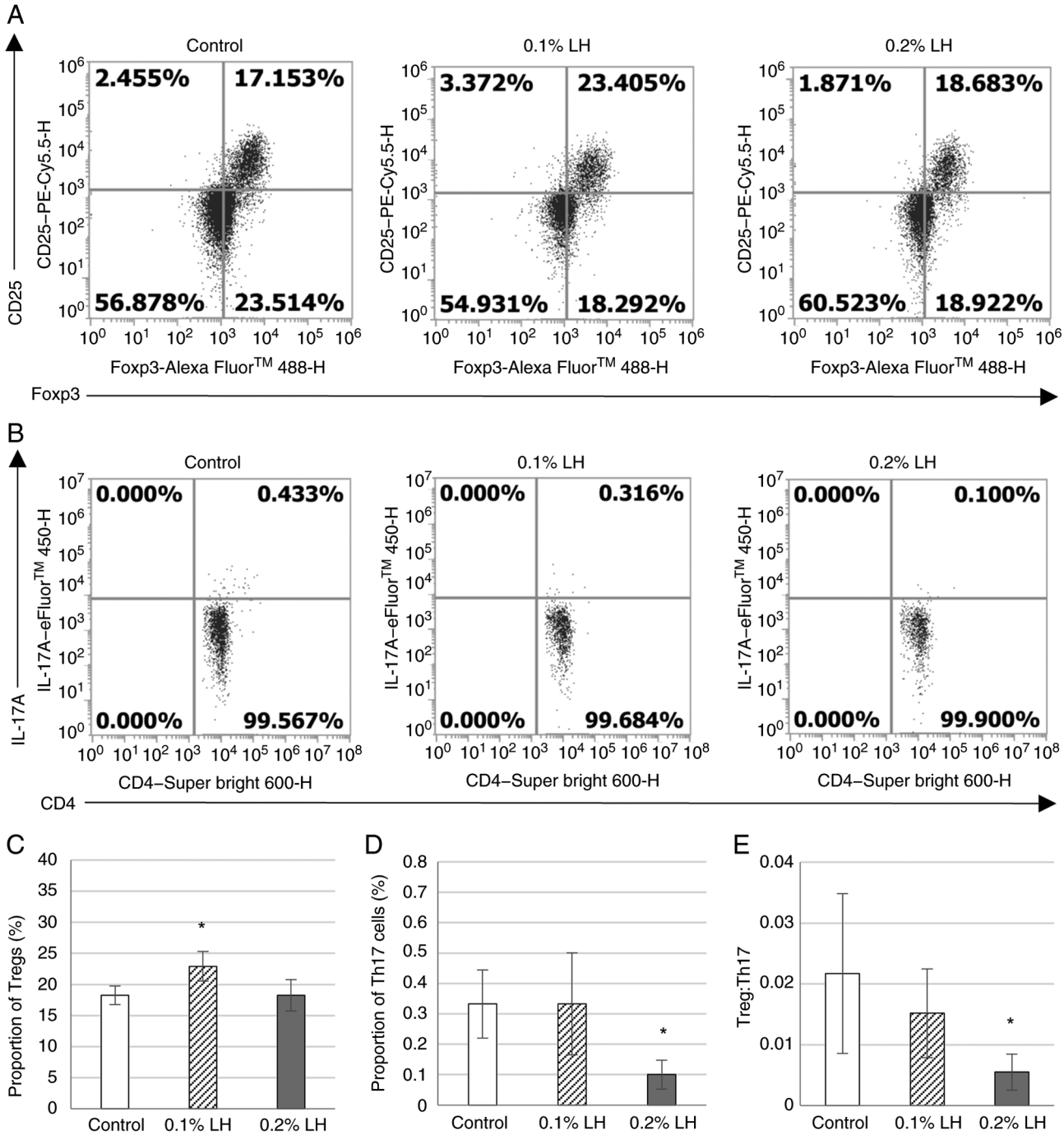

Figure 4. Effects of LH on Treg, Th17 and Th17/Treg ratio in the subcutaneous adipose tissue. Representative flow cytometric analysis of (A) Tregs ($CD25^+$ $Foxp3^+$) and (B) Th17 ($CD4^+$ $IL\text{-}17A^+$) cells in $CD4^+$ lymphocytes in the subcutaneous adipose tissue of 0.1 and 0.2% LH-exposed and control mice. Proportion of (C) Tregs and (D) Th17 cells. (E) Th17/Treg ratio $^*P<0.05$ compared with control. LH, *Lespedeza homoloba;* Treg, regulatory T; Th, T helper.

but there was no effect on mice exposed to 0.2% LH in the subcutaneous adipose tissue (Fig. 7C); no significant difference was observed in CTLA-4^+ Tregs in the spleen for either group (Fig. 7D).

LH-exposed mice exhibit increase $CD4^+$ T cells in spleen and decrease $CD8^+$ T cells in subcutaneous fat. To determine whether the significant increase in CTLA-4^+ Tregs induced by LH in subcutaneous adipose tissue affected expression of $CD4^+$ and $CD8^+$ T cells, the proportion of $CD4^+$ and $CD8^+$ T cells in was analyzed via flow cytometry. Mice exposed to 0.1% LH showed decreased $CD4^+$ T cells in the subcutaneous adipose tissue (Fig. 8A); however, in the spleen, $CD4^+$ T cells were increased in LH-exposed mice, significantly so in 0.2% LH-exposed mice (Fig. 8B). 0.1% LH-exposed mice had significantly decreased $CD8^+$ T cells in subcutaneous adipose tissue (Fig. 8C); however, in the spleen, no significant difference was observed in $CD8^+$ T cells (Fig. 8D).

Contents of LH with LT. (Fig. S1), peak areas of No. 1 and 2, 4, 8, 10, and 11 of LH were significantly higher than those of LT (Table SI). Formononetin, which is hydroxylated at the

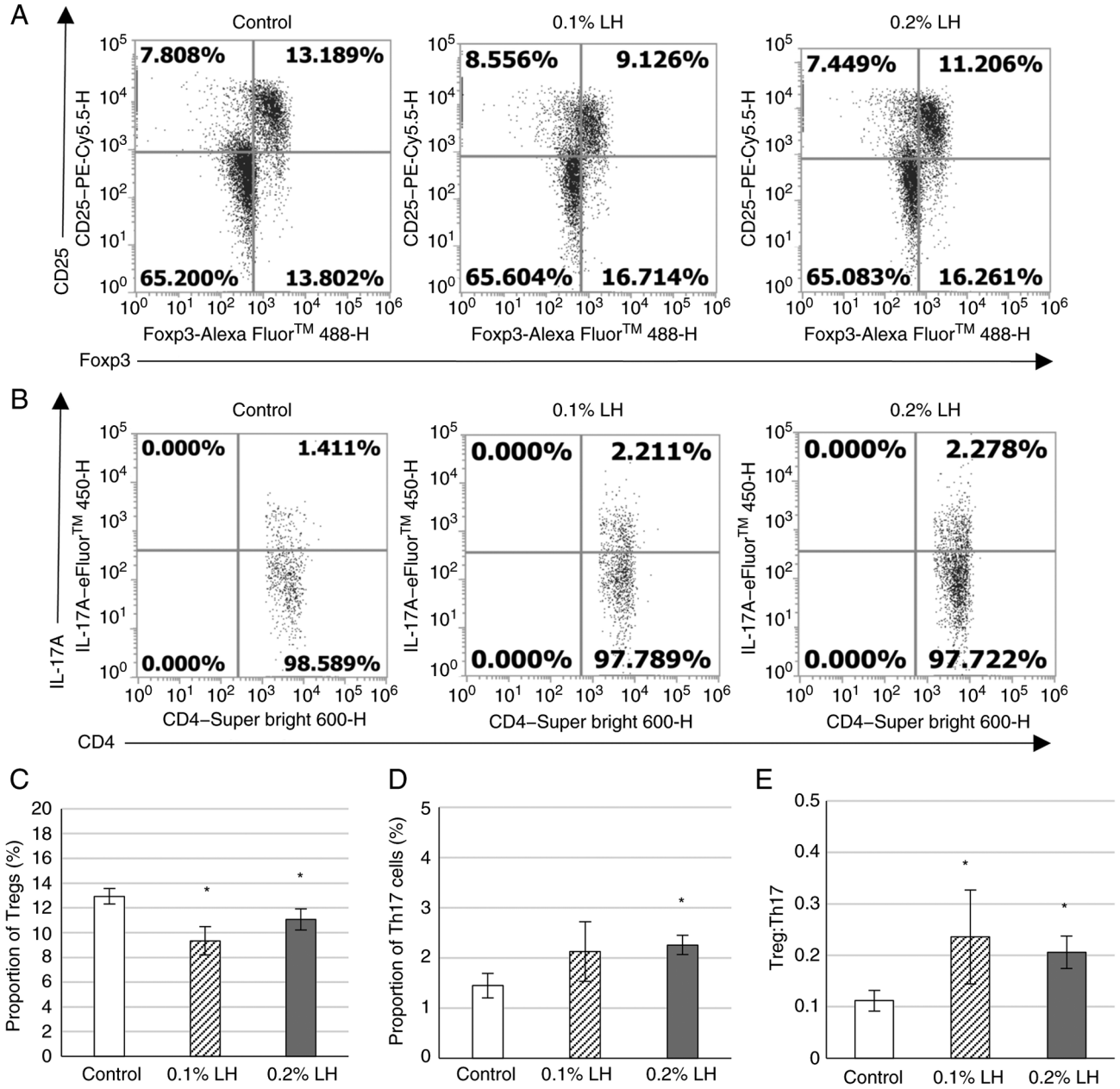

Figure 5. Effect of LH on Treg, Th17, and Th17/Treg ratio in the spleen. Representative flow cytometric analysis of (A) Tregs ($CD25^+$ $Foxp3^+$) and (B) Th17 ($CD4^+$ $IL\text{-}17A^+$) cells in $CD4^+$ lymphocytes in the spleen of 0.1 and 0.2% LH-exposed mice and control mice. Proportion of (C) Tregs and (D) Th17 cells. (E) Th17/Treg ratio. *P<0.05 vs. control. LH, *Lespedeza homoloba;* Treg, regulatory T; Th, T helper.

7-position and methylated at 4'-position of isoflavone, showed approximately 4 min of the retention time. Lespedezaflavanone H, which is prenylated at the 6-, 8-, and 2'-positions of flavanone, showed approximately 12 min of the retention time. Based on these results, LH and LT might contain low-polarity flavonoids, such as isoflavone or prenylated flavonoids. Although LH and LT contain almost similar components in the low-polarity flavonoids targeted in this study, the properties are thought to differ because of the difference in the content of these components.

Discussion

PPARγ is abundantly expressed in adipose tissue and modulates expression of proteins involved in lipid metabolism in adipocytes and adipogenesis. Thiazolidinediones (TZDs), including pioglitazone and rosiglitazone (PPARγ agonists), promote expression of adipogenic genes to differentiate preadipocytes into adipocytes (25), leading to adipocyte maturation (26). During adipocyte maturation, PPARγ activation increases expression of fatty acid transport protein (FATP) 1 and fatty acid-binding protein (FABP) 4, promoting fatty acid uptake and leading to accumulation of intracellular triglycerides in adipocytes (20). In adipocytes, PPARγ elevates expression of farnesoid X receptor gene, which induces expression of the stearoyl-CoA desaturase gene in the glucose metabolism pathway to accelerate fatty acid synthesis from glucose (27). PPARγ activation increases mitochondrial number and the expression of genes involved in mitochondrial β-oxidation (28). Here, LH significantly increased lipid

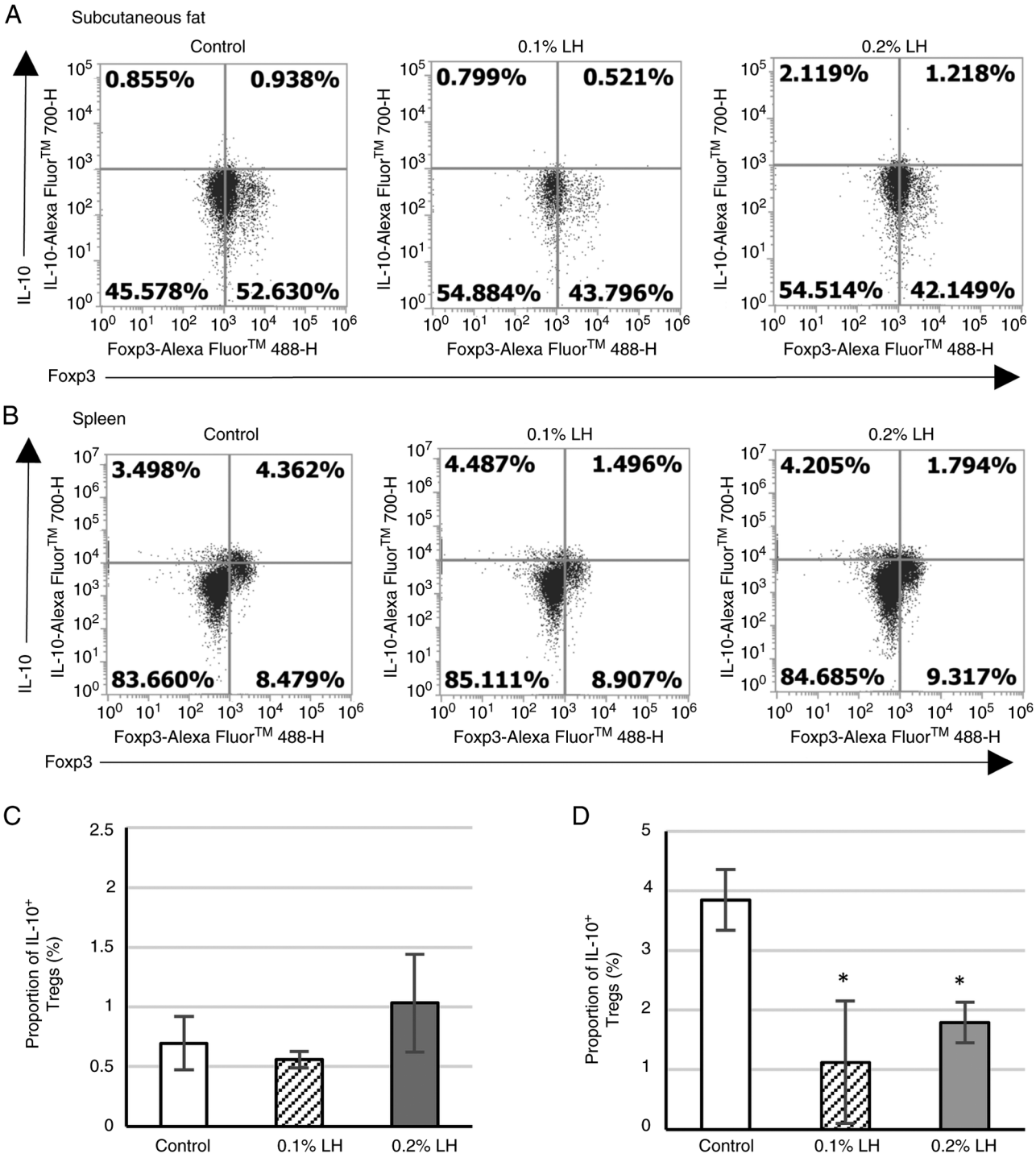

Figure 6. Effects of LH on IL-10$^+$ Tregs in the subcutaneous adipose tissue and spleen. Representative flow cytometric analysis of IL-10$^+$ Tregs (IL-10$^+$ Foxp3$^+$) in the subcutaneous (A) adipose tissue and (B) spleen. Proportion of IL-10$^+$ Tregs in (C) subcutaneous adipose tissue and (D) spleen. *P<0.05 vs. control. LH, *Lespedeza homoloba*; Treg, regulatory T.

accumulation in 3T3-L1-derived adipocytes and thus may increase the expression of FATP, FABP4 and mitochondria through its PPARγ agonistic activity leading to fatty acid accumulation in adipocytes.

Pioglitazone significantly decreased lipid accumulation in 3T3-L1-derived adipocytes at 0.28 μM. Similarly, in our previous study, rosiglitazone significantly reduced lipid accumulation in 3T3-L1-derived adipocytes (18). Rosiglitazone suppresses fibroblast proliferation via modulation of the p38 MAPK pathway, rather than by binding to PPARγ (29). This suggests that TZDs decrease the number of adipocytes differentiating from 3T3-L1 fibroblasts to decrease lipid accumulation. LH and LT exhibited an increase in PPARγ binding activity, promoting lipid accumulation in 3T3-L1-derived adipocytes, suggesting that they have no suppressive effect on fibroblast proliferation.

In mitochondria, the β-oxidation system generates reactive oxygen species (ROS). Hydrogen peroxide (H_2O_2), a mitochondrial-derived ROS, causes chronic inflammation;

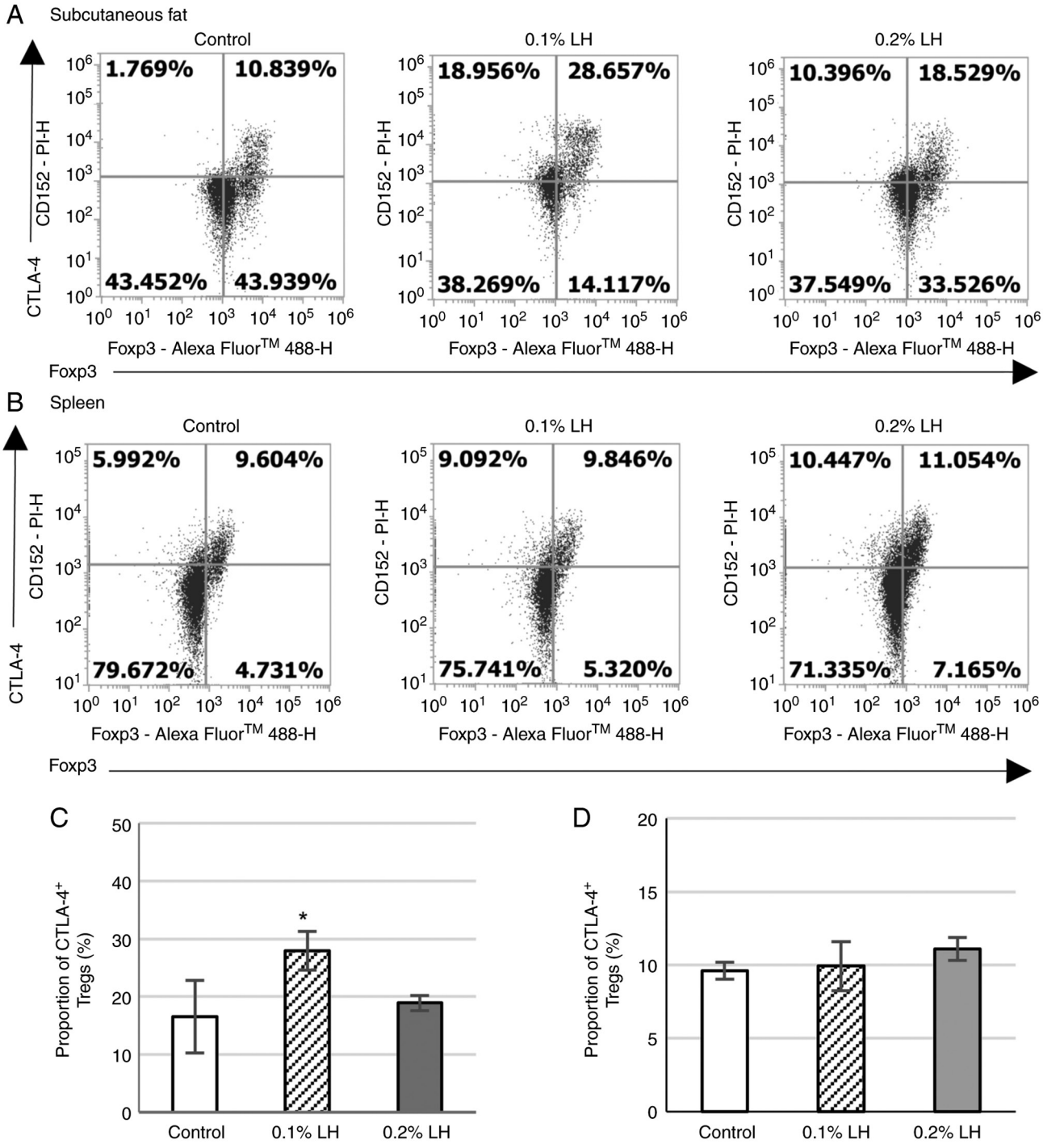

Figure 7. Effects of LH on CTLA-4$^+$ Treg in the subcutaneous adipose tissue and spleen. Representative flow cytometric analysis of CTLA-4$^+$ Treg (CTLA-4$^+$ Foxp3$^+$) cells in the subcutaneous (A) adipose tissue and (B) spleen. Proportion of CTLA-4$^+$ Tregs in (C) subcutaneous adipose tissue and (D) spleen. *P<0.05 vs. control. LH, *Lespedeza homoloba*; Treg, regulatory T.

it is converted to a hydroxy radical via transition metal catalysis, activating transcription factor NF-κB expressed in macrophages and promoting gene transcription of IL-1, IL-2, IL-6, IL-8, TNF-α, intercellular adhesion molecule-1, and inducible NO synthase, all of which contain NF-κB-binding sequences (25). In hypertrophied adipose tissue, chronic inflammation is induced by infiltration of macrophages that secrete proinflammatory cytokines. The activation of NF-κB, proinflammatory cytokines and inflammasomes increases risk of developing tissue inflammation and injury (30). Here, LH and LT exhibited significant binding activity to PPARγ. LH exhibited stronger DPPH radical scavenging activity than LT, which may enable it to scavenge excess superoxide anion and mitochondrial-derived ROS. This may prevent harmful events such as ferroptosis and pyroptosis in adipose tissue. Activation of PPARγ by the anti-diabetes compound rosiglitazone suppresses the production of the inflammatory cytokine IL-2 from intestinal tissue (31). Additionally, the present study revealed that LH suppressed IL-2 secretion from cultured splenocytes. PPARγ, activated by its agonist, promotes small

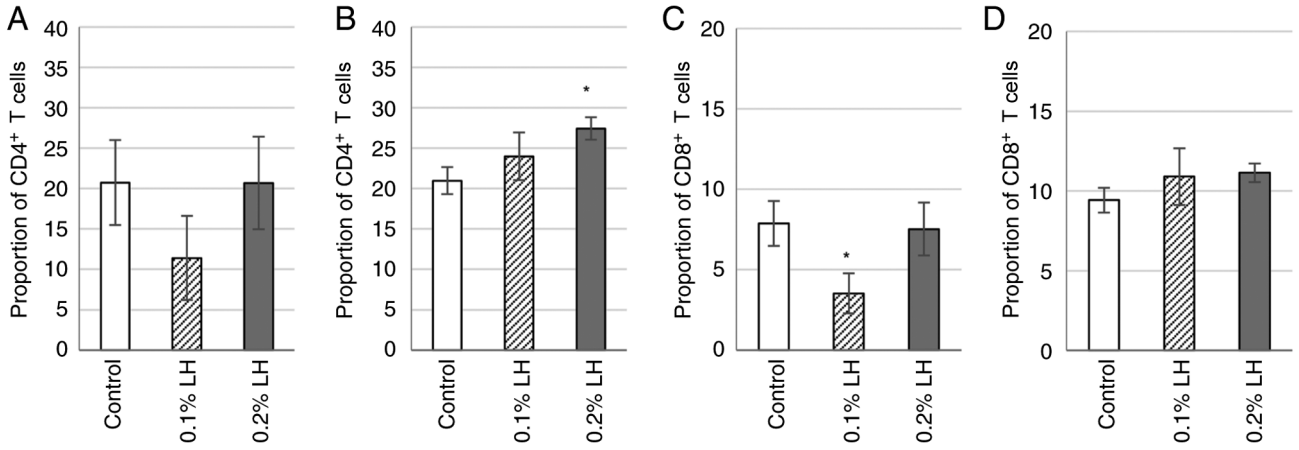

Figure 8. Effects of LH on CD4+ and CD8+ T cells in subcutaneous adipose tissue and spleen. Proportion of CD4+ T cells in the lymphocytes of (A) subcutaneous adipose tissue and (B) spleen and CD8+ T cells in the lymphocytes of (C) subcutaneous adipose tissue and (D) spleen. *P<0.05 vs. control. LH, *Lespedeza homoloba*.

ubiquitin-related modification (SUMOylation) and forms heterodimers with a DNA-bound repressor, leading to 19S proteasome-mediated degradation of the heterodimers, which inhibits expression of inflammatory cytokines (32). PPARγ SUMOylation increases insulin sensitivity in murine subcutaneous white adipose tissue (33). Therefore, LH is hypothesized to inhibit inflammation of adipose tissue as a PPARγ agonist and a radical scavenger by preventing expression of ROS and inflammatory cytokines.

Chronic activation of IL-1 receptors on pancreatic β-cells by IL-1β secreted from microglia induces pancreas dysfunction and T2D (34). In obesity, elevated the expression of IL-1β impairs insulin release, but IL-1 receptor antagonists treat T2D by increasing insulin secretion from the pancreas (34). Troglitazone, a PPARγ agonist, has been reported to suppress IL-1β synthesis in human monocytes (5), suggesting that PPARγ agonist may suppress T2D onset. Furthermore, the proinflammatory cytokine TNF-α is associated with insulin resistance and disrupts homeostasis of lipid and glucose metabolism (35). Additionally, PPARγ is expressed in macrophages and its agonist (an antidiabetic agent, troglitazone) inhibits the production of the inflammatory cytokine TNF-α in human monocytes (5). LH induced decreased TNF-α secretion from murine splenocytes compared with that of the control, although the difference was not statistically significant. PPARγ binding and radical scavenging activities of the present species from the genus *Lespedeza* were not strong enough to significantly reduce inflammatory factor TNF-α secretion from splenocytes.

The anti-inflammatory hormone adiponectin is synthesized almost exclusively in differentiated adipocytes and is present at high circulating levels. Adiponectin regulates blood glucose levels, lipid metabolism, and insulin sensitivity by binding to its receptors, adiponectin receptors 1 (AdipoR1) and 2 (AdipoR2). PPARγ agonist rosiglitazone promotes adiponectin transcription, synthesis and secretion of inguinal white adipose tissue (21). Here, the PPARγ agonist pioglitazone significantly increased adiponectin secretion from 3T3-L1-derived adipocytes at 28 and 280 μM (Fig. 2C). LH and LT both exhibited pronounced PPARγ ligand activity; however, increased adiponectin secretion from 3T3-L1-derived adipocytes was observed only in response to LH (Fig. 2D). These findings suggested that LH exerted a similar binding mechanism to the PPARγ agonist, thereby increasing adiponectin secretion from 3T3-L1-derived adipocytes.

The adipose tissue serves a crucial role in regulating insulin sensitivity (36). Macrophages and T cells migrate to hypertrophied adipose tissue with excess lipid accumulation, thereby activating inflammatory pathways (37). Chronic inflammation of adipose tissue caused by the migration of proinflammatory macrophages (M1) and T cells decreases glucose uptake (38) and impairs insulin signaling, leading to diabetes mellitus (39). An increase in number of Tregs prevents adipose tissue inflammation (40), and accumulation of Tregs in adipose tissue leads to improved insulin sensitivity in diabetes mellitus (41). CTLA-4, an immune checkpoint molecule expressed on Tregs, competes with CD28 on CD4+ T cells and binds to B7 on APCs, thereby expressing B7 on their surface; this process is referred to as trogocytosis. This suppresses APC function and decreases the number of CD4+ T cells. Treatment with CTLA-4Ig, a fusion protein that binds to B7, induces anti-inflammatory macrophage 2 polarization in adipose tissue (42). CD8+ T cells in adipose tissue serve a crucial role in macrophage infiltration and the initiation and propagation of adipose tissue inflammation (43). Th17 cells, characterized by production of proinflammatory cytokines such as IL-17A, IL-17F, IL-21, IL-22 and IL-26, promote adipose tissue inflammation (44). Th17/Treg imbalance initiates adipose tissue inflammation, leading to insulin resistance due to deficiency of Rab4b, an insulin-induced glucose transporter 4 translocation-controlling factor in adipocytes (24). The present study aimed to ascertain the effect of LH on the accumulation of Tregs, Th17 cells, and CD8+ T cells in adipose tissue using flow cytometric analysis. In the subcutaneous adipose tissue, LH induced a notable increase in Tregs and CTLA-4+ Tregs, along with a significant decrease in Th17 cells, the Th17/Treg ratio and CD8+ T cells. These findings suggested that LH shifted the Th17/Treg balance towards Treg dominance and decreased levels of CD4+ and CD8+ cells through trogocytosis by augmenting CTLA-4

on Tregs, thereby mitigating inflammation in subcutaneous adipose tissue.

A comparison of gene expression profiles between mouse visceral adipose tissue and lymph node Treg cells has revealed an upregulation of transcripts encoding PPARγ in mouse visceral adipose tissue Tregs (45). In addition, PPARγ activation by its agonist promotes Foxp3 gene transcription and induces effector Treg generation (46). Furthermore, intrinsic metabolic programming in immune cells is associated with immune cell differentiation and function (47,48). PPARγ agonist promotes the expression of CD36 and carnitine palmitoyl transferase I, which imports fatty acids into immune cells and enhances mitochondrial β-oxidation in the immune cell (49). Furthermore, in *in vitro* assay, PPARγ agonist increases $CD4^+$ $Foxp3^+$ Tregs generation from naïve $CD4^+$ T cells and boosts transcription of IL-10 and CTLA-4 of Tregs, indicating that PPARγ agonist promotes function of Tregs (49). These findings suggest that by PPARγ agonistic activity, LH may promote differentiation and function of Tregs in adipose tissue. By contrast with the subcutaneous adipose tissue, LH treatment in the spleen resulted in a substantial decrease in Tregs with a minimal effect on CTLA-4^+ Tregs, a notable increase in Th17 cells and the Th17/Treg ratio and an increasing trend in $CD8^+$ T cells. A splenic Treg population expressing low levels of PPARγ contains Treg precursors migrating to adipose tissue (50). Therefore, LH may promote Treg migration into subcutaneous adipose tissue from the spleen, thereby increasing the number of Th17 and $CD8^+$ T cells due to decreased Tregs in the spleen (Fig. 9).

Various mechanisms have been proposed for immunosuppressive mechanism of $Foxp3^+$ Tregs, including the anergy (immune unresponsiveness) of APC caused by CTLA-4 on Tregs, immunosuppression by immunosuppressive cytokines IL-10 and TGF-β secreted from Tregs and the suppression of inflammatory response via adenosine production by enzymes CD39/CD73 on Tregs. The adipose tissue of mice administered 0.1% LH showed a decrease in $CD4^+$ T cells due to an increase in CTLA-4^+ Tregs, thus inducing anergy in APCs. By contrast, the adipose tissue of mice administered 0.2% LH showed an increase in IL-10^+ Tregs. It has been reported that an increase in IL-10 in adipose tissue suppresses differentiation of naïve T cells into Th17 (51). Therefore, 0.2% LH was hypothesized to decrease Th17 cells owing to an increase in IL-10^+ Tregs and induce an immunosuppressive milieu in adipose tissue.

IL-10 serves various roles as an anti-inflammatory cytokine. Activation of the IL-10 signaling pathway in the intestine causes phosphorylated STAT3 (pSTAT3)-mediated anti-inflammatory response to induce epithelial cell proliferation, leading to healing of inflammatory bowel disease (52-54). In neurons and astrocytes, IL-10 promotes neurogenesis via the suppression of NF-κB signaling associated with the pSTAT3-mediated anti-inflammatory response in healing neuronal damage (55). In adipocytes, activation of the IL-10/STAT3 signaling cascade suppresses expression of thermogenic genes; thus, energy expenditure is limited (54). IL-10 ablation in white adipose tissue improves insulin sensitivity by increasing thermogenesis, energy expenditure and browning of white adipose tissue in mice (56). In humans, IL-10 is primarily produced by inflammatory immune cells in the white adipose tissue to promote insulin resistance (57).

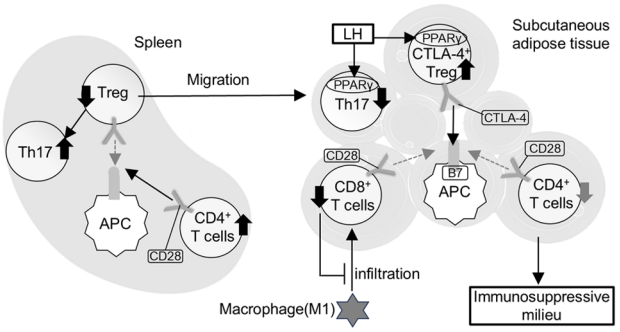

Figure 9 LH-induced immunosuppressive milieu in adipose tissue. LH stimulates PPARγ to increase CTLA-4 expression on Treg migrated from spleen, which decreases macrophage infiltration by decreasing levels of $CD8^+$ T cells. LH decreases Th17 cells by stimulating PPARγ, creating an immunosuppressive milieu in adipose tissue. LH, *Lespedeza homoloba*; PPARγ, peroxisome proliferator-activated receptor γ; APC, antigen-presenting cells; CTLA-4, cytotoxic T lymphocyte antigen 4; Treg, regulatory T cells.

AdipoR1 is expressed on Tregs (58) and adiponectin stimulation of AdipoR1 promotes secretion of the anti-inflammatory cytokine IL-10 from Tregs (59). In subcutaneous adipose tissue, IL-10^+ Tregs showed a decreasing trend in 0.1% LH-treated mice and an increasing trend in 0.2% LH-treated mice, similar to the trend observed for blood adiponectin levels. Additionally, blood glucose levels were higher in 0.2% LH-treated mice than in 0.1% LH-treated mice, suggesting that insulin sensitivity decreased with increasing IL-10^+ Tregs in adipose tissue. Furthermore, polyunsaturated fatty acids, endogenous ligands for nuclear retinoic acid receptor-related orphan receptor γ-expressed in Th17 cells, promote RORγt binding to IL-10 promoter region to increase IL-10 production from Th17 (60). Although cultured splenocytes of 0.1% LH-treated mice exhibited increased IL-10 secretion, mice exposed to 0.1 and 0.2% LH exhibited significantly decreased splenic IL-10^+ Tregs (Fig. 6D) and notably increased splenic Th17 cells. These findings suggest the possibility that LH increased IL-10 secretion from splenic Th17.

Elevated fasting glucose levels indicate a high risk of type 2 diabetes, whereas postprandial hyperglycemia indicates early-stage diabetes. Here, exposure to 0.1% LH in mice significantly decreased fasting blood glucose levels, which was accompanied by a substantial increase in number of CTLA-4^+ Tregs in subcutaneous adipose tissue. In 0.2% LH-treated mice, a significant decrease in fasting blood glucose levels was observed due to a notable decrease in Th17 cell number and Th17/Treg ratio in subcutaneous adipose tissue. Tregs improve glucose metabolism and insulin sensitivity in female mice by promoting subcutaneous adipose tissue browning and thermogenesis (61). PPARγ ligands, including rosiglitazone and pioglitazone, selectively suppress Th17 cell differentiation (62) and promote Treg differentiation (46). IL-17 knockout mice exhibit increased insulin sensitivity, glucose tolerance and serum adiponectin levels (63). These findings suggest that LH may prevent type 2 diabetes by increasing Tregs and decreasing Th17 cells in adipose tissue. Furthermore, to investigate whether LH generates an immunosuppressive milieu in adipose tissue of obese mice, 0.1% LH solution was administered for 30 days to male BALB/c mice which showed a significant increase in body weight after feeding high-fat diet for 8 weeks. The subcutaneous

adipose tissue was analyzed using flow cytometry. Although LH caused a slight decrease in Th17 cells, it did not affect Tregs (data not shown). Therefore, it was hypothesized that LH has no therapeutic effect on insulin resistance in obesity or diabetes.

LH, which is endemic to Japan, has been reported to exert a scavenging effect on superoxide anion radicals, chelae Fe^{2+}, which causes lipid peroxidation and exerts an antiallergic effect (64). Miyase *et al* (64,65) revealed that *Lespedeza* spp. are rich in isoflavones isoflav-3-en like haginin E and pterocarp-6a-en, which have hydroxyl groups at the C-3 and C-9 positions. Lespedezols E_1, A_6 and E_2, which are prenylated at the 8-, 10-, and 5'-positions of isoflavones, respectively, have also been isolated from LH. Miyase *et al* (64,65) reported that lipophilic isoflavone derivatives are active compounds among *Lespedeza* spp. because *Lespedeza* species can easily hybridize with other species of *Lespedeza* and biosynthesize similar constituents (64). Although the LH and LT used here may contain low-polarity flavonoids, such as isoflavones or prenylated flavonoids and contain similar constituents as shown in HPLC profiles, their properties are hypothesized to differ because of the difference in the content of these components. Prenylflavonoids are known to accumulate in high concentrations and persist for long periods in adipose tissue because of their high lipophilic properties (66). 8-prenylnaringenin, naringenin prenylated at the 8-position, has been suggested to have greater absorption in the body than naringenin and efficient accumulation in target tissue (9). Therefore, the prenylflavonoid constituents of LH may accumulate in adipose tissue and establish an anti-inflammatory environment, thereby improving insulin sensitivity and suppressing increased blood glucose levels.

LH activated nuclear receptor PPARγ, suggesting that components of LH permeated into the nucleus. Therefore, the adverse effects of long-term LH administration should be considered. Carnitine shuttle is key for mitochondrial fatty acid metabolism because the shuttle transport acyl moieties across the inner mitochondrial membrane for mitochondrial β-oxidation (67). However, TZDs, PPARγ agonists, may increase blood lipids levels by inhibiting the mitochondrial carnitine shuttle to inhibit mitochondrial β-oxidation, inducing cardiovascular risk (68). Among PPARγ agonists, rosiglitazone has been removed from the market because of adverse cardiovascular risk: Rosiglitazone therapy in 4,447 patients with type 2 diabetes was confirmed to increase risk of heart failure after 5 years of treatment (69), whereas pioglitazone significantly delayed the time to heart attack, acute coronary syndrome and stroke in 4,373 patients with type 2 diabetes following 4 years of treatment (70). The mechanism underlying the difference in cardiovascular risk development with PPARγ agonists remains unclear; however, long-term administration of PPARγ agonists must be considered for cardiovascular risk. However, administering 740 mg/day epimedium, which contains 48.2% prenylflavonoids, for 6 weeks in clinical trials did not show any adverse symptoms or significant changes in hepatic, hematological, or renal indices (71). These findings raise the possibility that LH, which mainly contains prenylflavonoids has less risk of cardiovascular disease for long-term administration.

The present study shows that LH exposure suppresses fasting blood glucose levels and suggests a mechanism that LH exerts a similar binding mechanism to the PPARγ agonist and promotes differentiation and function of Tregs by the activation of PPARγ expressed on the Tregs, which shifts Th17/Treg balance towards Treg dominance, thereby mitigating inflammation in subcutaneous adipose tissue. Prenylflavonoid constituents of LH are known to accumulate in high concentrations and persist for long periods in adipose tissue because of their high lipophilic properties and the constituents exhibited a strong binding to PPARγ. Therefore, LH is thought to establish an anti-inflammatory environment in adipose tissue to improve the function of adipose tissue.

Acknowledgements

The authors would like to thank Ms. Yukie Sato and Ms. Yu Ting Tang (Tohoku Medical and Pharmaceutical University, Sendai, Japan) for technical assistance with the experiments.

Funding

No funding was received.

Availability of data and materials

The data generated in the present study may be requested from the corresponding author.

Authors' contributions

KK conceived the study, designed and performed experiments, analyzed data and wrote and reviewed the manuscript. AT analyzed data and performed experiments. KS designed experiments and interpretation of data. KK and AT confirm the authenticity of all the raw data. KS made substantial contributions to supervision and validation. All authors have read and approved the final manuscript.

Ethics approval and consent to participate

All animal experiments were approved by Animal Experimental Committee of Tohoku Medical and Pharmaceutical University (approval no. 23032-a).

Patient consent for publication

Not applicable.

Competing interests

The authors declare that they have no competing interests.

References

1. Surmi BK and Hasty AH: Macrophage infiltration into adipose tissue: Initiation, propagation and remodeling. Future Lipidol 3: 545-556, 2008.
2. Olefsky JM and Glass CK: Macrophages, inflammation, and insulin resistance. Annu Rev Physiol 72: 219-246, 2010.
3. Shimobayashi M, Albert V, Woelnerhanssen B, Frei IC, Weissenberger D, Meyer-Gerspach AC, Clement N, Moes S, Colombi M, Meier JA, *et al*: Insulin resistance causes inflammation in adipose tissue. J Clin Invest 128: 1538-1550, 2018.

4. Lumeng CN, Bodzin JL and Saltiel AR: Obesity induces a phenotypic switch in adipose tissue macrophage polarization. J Clin Invest 117: 175-184, 2007.
5. Jiang C, Ting AT and Seed B: PPAR-gamma agonists inhibit production of monocyte inflammatory cytokines. Nature 391: 82-86, 1998.
6. Fooks AN, Beppu LY, Frias AB and D'Cruz LM: Adipose tissue regulatory T cells: Differentiation and function. Int Rev Immunol 42: 323-333, 2023.
7. Shen N, Wang T, Gan Q, Liu S, Wang L and Jin B: Plant flavonoids: Classification, distribution, biosynthesis, and antioxidant activity. Food Chem 383: 132531, 2022.
8. Yuan D, Guo Y, Pu F, Yang C, Xiao X, Du H, He J and Lu S: Opportunities and challenges in enhancing the bioavailability and bioactivity of dietary flavonoids: A novel delivery system perspective. Food Chem 430: 137115, 2024.
9. Mukai R, Fujikura Y, Murota K, Uehara M, Minekawa S, Matsui N, Kawamura T, Nemoto H and Terao J: Prenylation enhances quercetin uptake and reduces efflux in Caco-2 cells and enhances tissue accumulation in mice fed long-term. J Nutr 143: 1558-1564, 2013.
10. American Veterinary Medical Association (AVMA): AVMA guidelines for the euthanasia of animals: 2020 edition. American Veterinary Medical Association, Schaumburg, IL, 2020.
11. Lee SJ, Hossaine MDA and Park SC: A potential anti-inflammation activity and depigmentation effect of *Lespedeza* bicolor extract and its fractions. Saudi J Biol Sci 23: 9-14, 2016.
12. Mariadoss AVA, Park S, Saravanakumar K, Sathiyaseelan A and Wang MH: Phytochemical profiling, in vitro antioxidants, and antidiabetic efficacy of ethyl acetate fraction of *Lespedeza cuneata* on streptozotocin-induced diabetic rats. Environ Sci Pollut Res Int 30: 60976-60993, 2023.
13. Kim NK, Park HM, Lee J, Ku KM and Lee CH: Seasonal Variations of metabolome and tyrosinase inhibitory activity of *Lespedeza maximowiczii* during growth periods. J Agric Food Chem 63: 8631-8639, 2015.
14. Bae J, Lee D, Lee TK, Song JH, Lee JS, Lee S, Yoo SW, Kang KS, Moon E, Lee S and Kim KH: (-)-9'-O-(α-l-Rhamnopyranosyl) lyoniresinol from *Lespedeza cuneata* suppresses ovarian cancer cell proliferation through induction of apoptosis. Bioorg Med Chem Lett 28: 122-128, 2018.
15. Lee JH, Parveen A, Do MH, Lim Y, Shim SH and Kim SY: *Lespedeza cuneata* protects the endothelial dysfunction via eNOS phosphorylation of PI3K/Akt signaling pathway in HUVECs. Phytomedicine 48: 1-9, 2018.
16. Konno T, Sasaki K, Kobayashi K and Murata T: Indirubin promotes adipocyte differentiation and reduces lipid accumulation in 3T3-L1 cells via peroxisome proliferator-activated receptor γ activation. Mol Med Rep 21: 1552-1560, 2020.
17. Blois MS: Antioxidant determinations by the use of a stable free radical. Nature 181: 1199-1200, 1958.
18. Kobayashi K, Tang YT and Sasaki K: Paeoniflorin, a constituent of Kami-shoyo-san, suppresses blood glucose levels in postmenopausal diabetic mice by promoting the secretion of estradiol from adipocytes. Biochem Biophys Rep 32: 101335, 2022.
19. Daynes RA and Jones DC: Emerging roles of PPARS in inflammation and immunity. Nat Rev Immunol 2: 748-759, 2002.
20. Hardwick JP, Osei-Hyiaman D, Wiland H, Abdelmegeed MA and Song BJ: PPAR/RXR regulation of fatty acid metabolism and fatty acid omega-hydroxylase (CYP4) isozymes: Implications for prevention of lipotoxicity in fatty liver disease. PPAR Res 2009: 952734, 2009.
21. Andrade ML, Gilio GR, Perandini LA, Peixoto AS, Moreno MF, Castro É, Oliveira TE, Vieira TS, Ortiz-Silva M, Thomazelli CA, *et al*: PPARγ-induced upregulation of subcutaneous fat adiponectin secretion, glyceroneogenesis and BCAA oxidation requires mTORC1 activity. Biochim Biophys Acta Mol Cell Biol Lipids 1866: 158967, 2021.
22. Wu Z, Xie Y, Morrison RF, Bucher NL and Farmer SR: PPARgamma induces the insulin-dependent glucose transporter GLUT4 in the absence of C/EBPalpha during the conversion of 3T3 fibroblasts into adipocytes. J Clin Invest 101: 22-32, 1998.
23. Way JM, Harrington WW, Kathleen KB, Gottschalk WK, Sundseth SS, Mansfield TA, Ramachandran RK, Willson TM and Kliewer SA: Comprehensive messenger ribonucleic acid profiling reveals that peroxisome proliferator-activated receptor gamma activation has coordinate effects on gene expression in multiple insulin-sensitive tissues. Endocrinology 142: 1269-1277, 2001.
24. Gilleron J, Bouget G, Ivanov S, Meziat C, Ceppo F, Vergoni B, Djedaini M, Soprani A, Dumas K, Jacquel A, *et al*: Rab4b deficiency in T cells promotes adipose Treg/Th17 imbalance, adipose tissue dysfunction, and insulin resistance. Cell Rep 25: 3329-3341.e5, 2018.
25. Oliveira-Marques V, Marinho HS, Cyrne L and Antunes F: Modulation of NF-kappaB-dependent gene expression by H_2O_2: A major role for a simple chemical process in a complex biological response. Antioxid Redox Signal 11: 2043-2053, 2009.
26. Sun C, Mao S, Chen S, Zhang W and Liu C: PPARs-orchestrated metabolic homeostasis in the adipose tissue. Int J Mol Sci 22: 8974, 2021.
27. Shinohara S and Fujimori K: Promotion of lipogenesis by PPARγ-activated FXR expression in adipocytes. Biochem Biophys Res Commun 527: 49-55, 2020.
28. Bogacka I, Ukropcova B, McNeil M, Gimble JM and Smith SR: Structural and functional consequences of mitochondrial biogenesis in human adipocytes in vitro. J Clin Endocrinol Metab 90: 6650-6656, 2005.
29. Antonelli A, Ferri C, Ferrari SM, Colaci M, Ruffilli I, Sebastiani M and Fallahi P: Peroxisome proliferator-activated receptor γ agonists reduce cell proliferation and viability and increase apoptosis in systemic sclerosis fibroblasts. Br J Dermatol 168: 129-135, 2013.
30. Mittal M, Siddiqui MR, Tran K, Reddy SP and Malik AB: Reactive oxygen species in inflammation and tissue injury. Antioxid Redox Signal 20: 1126-1167, 2014.
31. Yu D, Liu JQ, Mo LH, Luo XQ, Liu ZQ, Wu GH, Yang LT, Liu DB, Wang S, Liu ZG and Yang PC: Specific antigen-guiding exosomes inhibit food allergies by inducing regulatory T cells. Immunol Cell Biol 98: 639-649, 2020.
32. Martin H: Role of PPAR-gamma in inflammation. Prospects for therapeutic intervention by food components. Mutat Res 690: 57-63, 2010.
33. Katafuchi T, Holland WL, Kollipara RK, Kittler R, Mangelsdorf DJ and Kliewer SA: PPARγ-K107 SUMOylation regulates insulin sensitivity but not adiposity in mice. Proc Natl Acad Sci USA 115: 12102-12111, 2018.
34. Wiedemann SJ, Trimigliozzi K, Dror E, Meier DT, Molina-Tijeras JA, Rachid L, Foll CL, Magnan C, Schulze F, Stawiski M, *et al*: The cephalic phase of insulin release is modulated by IL-1β. Cell Metab 34: 991-1003,e6, 2022.
35. Cawthorn WP and Sethi JK: TNF-alpha and adipocyte biology. FEBS Lett 582: 117-131, 2008.
36. Smith U and Kahn BB: Adipose tissue regulates insulin sensitivity: Role of adipogenesis, de novo lipogenesis and novel lipids. J Inter Med 280: 465-475, 2016.
37. Weisberg SP, McCann D, Desai M, Rosenbaum M, Leibel RL and Ferrante AW Jr: Obesity is associated with macrophage accumulation in adipose tissue. J Clin Invest 112: 1796-1808, 2003.
38. Carey AL, Steinberg GR, Macaulay SL, Thomas WG, Holmes AG, Ramm G, Prelovsek O, Hohnen-Behrens C, Watt MJ, James DE, *et al*: Interleukin-6 increases insulin-stimulated glucose disposal in humans and glucose uptake and fatty acid oxidation in vitro via AMP-activated protein kinase. Diabetes 55: 2688-2697, 2006.
39. Uysal KT, Wiesbrock SM, Marino MW and Hotamisligil GS: Protection from obesity-induced insulin resistance in mice lacking TNF-alpha function. Nature 389: 610-614, 1997.
40. Lumeng CN, Maillard I and Saltiel AR: T-ing up inflammation in fat. Nat Med 15: 846-847, 2009.
41. Chen LW, Chen PH, Tang CH and Yen JH: Adipose-derived stromal cells reverse insulin resistance through inhibition of M1 expression in a type 2 diabetes mellitus mouse model. Stem Cell Re Ther 13: 357, 2022.
42. Fujii M, Inoguchi T, Batchuluun B, Sugiyama N, Kobayashi K, Sonoda N and Takayanagi R: CTLA-4Ig immunotherapy of obesity-induced insulin resistance by manipulation of macrophage polarization in adipose tissues. Biochem Biophys Res Commun 438: 103-109, 2013.
43. Nishimura S, Manabe I, Nagasaki M, Eto K, Yamashita H, Ohsugi M, Otsu M, Hara K, Ueki K, Sugiura S, *et al*: CD8+ effector T cells contribute to macrophage recruitment and adipose tissue inflammation in obesity. Nature Med 15: 914-920, 2009.
44. Shin JH Shin DW and Noh M: Interleukin-17A inhibits adipocyte differentiation in human mesenchymal stem cells and regulates pro-inflammatory responses in adipocytes. Biochem Pharmacol 77: 1835-1844, 2009.

45. Cipolletta D, Feuerer M, Li A, Kamei N, Lee J, Shoelson SE, Benoist C and Mathis D: PPAR-γ is a major driver of the accumulation and phenotype of adipose tissue Treg cells. Nature 486: 549-553, 2012.
46. Lei J, Hasegawa H, Matsumoto T and Yasukawa M: Peroxisome proliferator-activated receptor α and γ agonists together with TGF-β convert human CD4+CD25-T cells into functional Foxp3+ regulatory T cells. J Immunol 185: 7186-7198, 2010.
47. Sun L, Fu J and Zhou Y: Metabolism controls the balance of Th17/T-regulatory cells. Front Immunol 8: 1632, 2017.
48. Maciolek JA, Pasternak JA and Wilson HL: Metabolism of activated T lymphocytes. Curr Opin Immunol 27: 60-74, 2014.
49. Miao Y, Zhang C, Yang L, Zeng X, Hu Y, Xue X, Dai Y and Wei Z: The activation of PPARγ enhances Treg responses through up-regulating CD36/CPT1-mediated fatty acid oxidation and subsequent N-glycan branching of TβRII/IL-2Rα. Cell Commun Signal 20: 48, 2022.
50. Li C, Muñoz-Rojas AR, Wang G, Mann AO, Benoist C and Mathis D: PPARγ marks splenic precursors of multiple nonlymphoid-tissue Treg compartments. Proc Natl Acad Sci USA 118: e2025197118, 2021.
51. Jeong W, Jung JY, Kim SC and Im WT: Ginsenoside F2 for prophylaxis and treatment of liver disease. European patent EP2992933A1. Filed September 4, 2015; issued March 9, 2016.
52. Lin Z, Wang Z, Hegarty JP, Lin TR, Wang Y, Deiling S, Wu R, Thomas NJ and Floros J: Genetic association and epistatic interaction of the interleukin-10 signaling pathway in pediatric inflammatory bowel disease. World J Gastroenterol 23: 4897-4909, 2017.
53. Fay NC, Muthusamy BP, Nyugen LP, Desai RC, Taverner A, MacKay J, Seung M, Hunter T, Liu K, Chandalia A, *et al*: A novel fusion of IL-10 engineered to traffic across intestinal epithelium to treat colitis. J Immunol 205: 3191-3204, 2020.
54. Saraiva M, Vieira P and O'Garra A: Biology and therapeutic potential of interleukin-10. J Exp Med 217: e20190418, 2020.
55. Vidal PM, Lemmens E, Dooley D and Hendrix S: The role of 'anti-inflammatory' cytokines in axon regeneration. Cytokine Growth Factor Rev 24: 1-12, 2013.
56. Rajbhandari P, Thomas BJ, Feng AC, Hong C, Wang J, Vergnes L, Sallam T, Wang B, Sandhu J, Seldin MM, *et al*: IL-10 signaling remodels adipose chromatin architecture to limit thermogenesis and energy expenditure. Cell 172: 218-233.e17, 2018.
57. Acosta JR, Tavira B, Douagi I, Kulyté A, Arner P, Rydén M and Laurencikiene J: Human-specific function of IL-10 in adipose tissue linked to insulin resistance. J Clin Endocrinol Metab 104: 4552-4562, 2019.
58. Ramos-Ramírez P, Malmhäll C, Johansson K, Lötvall J and Bossios A: Weight gain alters adiponectin receptor 1 expression on adipose tissue-resident helios+ regulatory T cells. Scand J Immunol 83: 244-254, 2016.
59. Ramos-Ramirez P, Malmhäl C, Tliba O, Rådinger M and Bossios A: Adiponectin/AdipoR1 axis promotes IL-10 release by human regulatory T cells. Front Immunol 12: 677550, 2021.
60. Wu X, Tian J and Wang S: Insight into non-pathogenic Th17 cells in autoimmune diseases. Front Immunol 9: 1112, 2018.
61. Fang W, Deng Z, Benadjaoud F, Yang D, Yang C and Shi GP: Regulatory T cells promote adipocyte beiging in subcutaneous adipose tissue. FASEB J 34: 9755-9770, 2020.
62. Klotz L, Burgdorf S, Dani I, Saijo K, Flossdorf J, Hucke S, Alferink J, Novak N, Beyer M, Mayer G, *et al*: The nuclear receptor PPAR gamma selectively inhibits Th17 differentiation in a T cell-intrinsic fashion and suppresses CNS autoimmunity. J Exp Med 206: 2079-2089, 2009.
63. Chang YC, Hee SW and Chuang LM: T helper 17 cells: A new actor on the stage of type 2 diabetes and aging? J Diabetes Investig 12: 909-913, 2021.
64. Miyase T, Sano M, Nakai H, Muraoka M, Nakazawa M, Suzuki M, Yoshino K, Nishihara Y and Tanai J: Antioxidants from *Lespedeza homoloba*. (I). Phytochemistry 52: 303-310, 1999.
65. Miyase T, Sano M, Yoshio K and Nonaka K: Antioxidants from *Lespedeza homoloba* (II). Phytochemistry 52: 311-319, 1999.
66. Terao J and Mukai R: Prenylation modulates the bioavailability and bioaccumulation of dietary flavonoids. Arch Biochem Biophys 559: 12-16, 2014.
67. Longo N, Frigeni M and Pasquali M: Carnitine transport and fatty acid oxidation. Biochem Biophys Acta 1863: 2422-2435, 2016.
68. Sultan AA, Rattray Z and Rattray NJW: Toxicometabolomics-based cardiotoxicity evaluation of Thiazolidinedione exposure in human-derived cardiomyocytes. Metabolomics 20: 24, 2024.
69. Home PD, Pocock SJ, Beck-Nielsen H, Curtis PS, Gomis R, Hanefeld M, Jones NP, Komajda M and McMurray JJ; RECORD Study Team: Rosiglitazone evaluated for cardiovascular outcomes in oral agent combination therapy for type 2 diabetes (RECORD): A multicentre, randomised, open-label trial. Lancet 373: 2125-2135, 2009.
70. Dormandy JA, Charbonnel B, Eckland DJA, Erdmann E, Massi-Benedetti M, Moules IK, Skene AM, Tan MH, Lefèbvre PJ, Murray GD, *et al*: Secondary prevention of macrovascular events in patients with type 2 diabetes in the PROactive study (PROspective pioglitAzone clinical trial in macroVascular events): A randomised controlled trial. Lancet 366: 1279-1289, 2005.
71. Yong EL, Cheong WF, Huang Z, Thu WPP, Cazenave-Gassiot A, Seng KY and Logan S: Randomized, double-blind, placebo-controlled trial to examine the safety, pharmacokinetics and effects of epimedium prenylflavonoids, on bone specific alkaline phosphatase and the osteoclast adaptor protein TRAF6 in post-menopausal women. Phytomedicine 91: 153680, 2021.

Copyright © 2024 Kobayashi et al. This work is licensed under a Creative Commons Attribution-NonCommercial-NoDerivatives 4.0 International (CC BY-NC-ND 4.0) License.